Cooperativity of the N- and C-Terminal Domains of Insulin-like Growth Factor (IGF) Binding Protein 2 in IGF Binding†

Zhihe Kuang,‡,§ Shenggen Yao,‡ Kerrie A. McNeil,§ Julian A. Thompson,|| Leon A. Bach,|| Briony E. Forbes,§ John C. Wallace,§ and Raymond S. Norton*,‡

The Walter and Eliza Hall Institute of Medical Research, 1G Royal Parade, Parkville 3050, Australia, School of Molecular and Biomedical Science, The University of Adelaide, Adelaide 5005, Australia, and Department of Medicine, Monash University, and Department of Endocrinology and Diabetes, Alfred Hospital, Melbourne 3004, Australia

Received June 25, 2007; Revised Manuscript Received September 18, 2007

ABSTRACT: A family of six insulin-like growth factor (IGF) binding proteins (IGFBP-1−6) binds IGF-I and IGF-II with high affinity and thus regulates their bioavailability and biological functions. IGFBPs consist of N- and C-terminal domains, which are highly conserved and cysteine-rich, joined by a variable linker domain. The role of the C-domain in IGF binding is not completely understood in that C-domain fragments have very low or even undetectable IGF binding affinity, but loss of the C-domain dramatically disrupts IGF binding by IGFBPs. We recently reported the solution structure and backbone dynamics of the C-domain of IGFBP-2 (C-BP-2) and identified a pH-dependent heparin binding site [Kuang, Z., Yao, S., Keizer, D. W., Wang, C. C., Bach, L. A., Forbes, B. E., Wallace, J. C., and Norton, R. S. (2006) Structure, dynamics and heparin binding of the C-terminal domain of insulin-like growth factor-binding protein-2 (IGFBP-2), *J. Mol. Biol. 364*, 690−704]. Here, we have analyzed the molecular interactions among the N-domain of IGFBP-2 (N-BP-2), C-BP-2, and IGFs using cross-linking and nuclear magnetic resonance (NMR) spectroscopy. The binding of C-BP-2 to the IGF-I·N-BP-2 binary complex was significantly stronger than the binding of C-BP-2 to IGF-I alone, switching from intermediate exchange to slow exchange on the NMR time scale. A conformational change or stabilization of the IGF-I Phe49−Leu54 region and the Phe49 aromatic ring upon binding to the N-domains, as well as an interdomain interaction between N-BP-2 and C-BP-2 (which is also detectable in the absence of ligand), may contribute to this cooperativity in IGF binding. Glycosaminoglycan binding by IGFBPs can affect their IGF binding although the effects appear to differ among different IGFBPs; here, we found that heparin bound to the IGF-I·N-BP-2·C-BP-2 ternary complex, but did not cause it to dissociate.

The insulin-like growth factor (IGF)[1] system is an important growth regulatory system in vertebrates. Proper functioning of the IGF system is essential for prenatal and postnatal growth and development, whereas abnormalities of the system are associated with many diseases such as growth disorders, diabetes, and cancer (*1*, *2*). IGF-I and -II, the ligands in this system, are polypeptide hormones that exert mitogenic and metabolic effects via IGF and insulin receptors. The bioavailability and cellular actions of IGFs are tightly regulated by a family of six high-affinity IGF binding proteins (IGFBP-1 to IGFBP-6) (*3*−*6*). The majority of the IGFs in the circulation or extracellular space are present in the IGFBP-bound form. Because IGF·IGFBP complexes cannot activate the IGF-I receptor, binding to IGFBPs generally inhibits IGF actions. In certain situations, however, IGFBPs can also enhance IGF actions by incompletely understood mechanisms; for instance, IGFBPs may localize IGF molecules to the receptor-abundant cell surface and promote the subsequent release of IGFs (*3*).

IGFBPs consist of three domains of approximately equal length, with highly conserved and cysteine-rich N- and C-terminal domains joined by a variable linker domain (*5*, *6*). There are intradomain disulfide bonds within the N- or C-domains but no interdomain disulfide bonds (*6*). Both the N- and C-domains of IGFBPs are required for high-affinity IGF binding, as isolated N- and C-domain fragments have significantly lower affinities than full-length IGFBPs (*3*−*10*). The IGF binding sites on the IGFBP N- and C-domains, as well as the IGFBP binding sites on IGFs, have been mapped using various approaches (*11*−*18*). Three-dimensional structures for IGFBP N- and C-domains have been solved (*19*−*25*), but the structure of a full-length IGFBP, either alone or in complex with IGF, has not yet been determined. We have reported the solution structure

† This work was supported in part by an Australian Research Council Discovery Grant (DP0449906). Z.K. acknowledges receipt of an International Postgraduate Research Scholarship (IPRS) from the University of Adelaide.

* To whom correspondence should be addressed. E-mail: ray.norton@wehi.edu.au. Fax: +61 3 9345 2686. Phone +61 3 9345 2306.

‡ The Walter and Eliza Hall Institute of Medical Research.

§ The University of Adelaide.

|| Monash University and Alfred Hospital.

[1] Abbreviations: C-BP-2, C-terminal domain of insulin-like growth factor binding protein 2; DTT, dithiothreitol; HSQC, heteronuclear single-quantum coherence; IGF, insulin-like growth factor; IGFBP, insulin-like growth factor binding protein; N-BP-2, N-terminal domain of insulin-like growth factor binding protein 2; NMR, nuclear magnetic resonance; PBS, phosphate-buffered saline; PCR, polymerase chain reaction; HPLC, high-performance liquid chromatography.

10.1021/bi701251d CCC: $37.00
Published on Web 11/07/2007

and backbone dynamics of the C-domain of IGFBP-2 (C-BP-2) and identified a pH-dependent heparin binding site on C-BP-2 (*24*).

The reported affinities of IGFs for both naturally occurring and recombinant C-domain fragments vary greatly. Losses of affinity from as little as 10-fold to as much as 2000-fold compared to the respective full-length proteins have been reported for different C-domain fragments (*8*, *9*, *26*−*29*). In some cases the IGF binding affinity of C-domains was too low to be detected, including that of C-BP-4 using solution binding assay (*30*), isothermal titration calorimetry and nuclear magnetic resonance (NMR) spectroscopy (*21*), or analytical ultracentrifugation (*31*), and that of C-BP-5 using BIAcore (*19*).

To clarify the role of the C-domain in IGF binding, we have analyzed the molecular interactions among the IGFBP-2 N-domain (N-BP-2), C-BP-2, and IGFs using affinity cross-linking and NMR spectroscopy. We found that the binding of C-BP-2 to the IGF-I·N-BP-2 binary complex was significantly stronger than its binding to IGF-I alone. A conformational change or stabilization of the Phe49−Leu54 region of IGF-I upon binding to the N-domain, as well as an interdomain interaction between N-BP-2 and C-BP-2, may contribute to this cooperativity between the N- and C-domains in IGF binding. Our findings highlight the need to take a global approach to studying protein interactions when more than one domain contributes to the formation of a high-affinity complex, as synergistic conformational changes and interdomain interactions can influence the overall interaction.

IGFBP-3 and IGFBP-5 also bind glycosaminoglycans, and this interaction is important for the modulation of IGF actions (*3*). However, the role of glycosaminoglycan binding in modulation of IGF action by IGFBP-2 is controversial (*32*−*34*). Here we show that low molecular weight heparin bound to the IGF-I·N-BP-2·C-BP-2 ternary complex but did not dissociate that complex.

EXPERIMENTAL PROCEDURES

Preparation of $^{15}N/^{13}C$-Labeled IGF-I. The human IGF-I expression vector was developed by King et al. (*35*). The IGF-I construct was transformed into *Escherichia coli* JM101 and grown on minimal medium containing 1.6 g L^{-1} $^{15}NH_4Cl$ and 5 g L^{-1} $^{13}C_6$-glucose in a 3 L Applikon fermenter. Expression was induced with 100 μM isopropyl β-D-thiogalactoside, and additional 1.6 g L^{-1} $^{15}NH_4Cl$ and 2.5 g L^{-1} $^{13}C_6$-glucose were added at this time. Inclusion bodies containing the IGF-I linked to an N-terminal [Met1]-pGH extension peptide were isolated using a French press and then solubilized as a 10% (w/v) solution in 8 M urea, 0.1 M Tris, 40 mM glycine, and 20 mM dithiothreitol (DTT), pH 9.1. Refolding was achieved by diluting the reduced inclusion bodies in a final concentration of 2 M urea, 100 mM Tris, 10 mM glycine, 5 mM EDTA, 0.4 mM DTT, and 1 mM 2-hydroxylethyl disulfide, pH 9.1. After slow stirring for 90 min at room temperature, the reaction was stopped by acidification to pH 2.5 with HCl. The refolding was monitored by reversed-phase HPLC. The folded IGF-I was concentrated on a 16 mm × 100 mm Sepharose Fast Flow S column (GE Healthcare) equilibrated with 8 M urea and 50 mM sodium acetate, pH 4.8, and eluted with 8 M urea, 1 M NaCl, and 50 mM sodium acetate, pH 4.8. The fusion protein was cleaved by diluting the ion exchange fraction in a solution containing 2 M urea and 1 M hydroxylamine−HCl, pH 8.5 (adjusted with LiOH), to a final protein concentration of 0.2 mg/mL. The cleavage reaction was performed at 37 °C for 20 h and terminated by acidification to pH 2.5 with HCl. Final purification was achieved by reversed-phase HPLC on a 10 mm × 250 mm C4 Vydac (300 Å pore size, 10 μm bead size) column equilibrated with 22% (v/v) acetonitrile and 0.1% (v/v) TFA. IGF-I was eluted by applying a linear gradient from 22% to 44% (v/v) acetonitrile in 0.1% (v/v) TFA over 210 min at a flow rate of 5 mL/min. Mass spectrometry confirmed that the isotope incorporation efficiency was >98%.

Preparation of Unlabeled and ^{15}N-Labeled IGFBP-2 Domain Fragments. Expression and purification of unlabeled and ^{15}N-labeled C-BP-2 ($^{183-289}$IGFBP-2) samples have been described (*24*). N-BP-2 ($^{1-138}$IGFBP-2) samples were prepared using a method similar to that described for the production of C-BP-2 (*24*). In brief, a cDNA encoding residues 1−138 of human IGFBP-2 and a 3C protease cleavage site at its N-terminus was synthesized by PCR, using the forward primer 5′-TTTTTTCCATGGCACTGGAAGTTCTGTTCCAGGGGCCCGAGGTGCTGTTCCGCTGCCC-3′ and the reverse primer 5′-TTTTACGAATTCTTAGCCTCCCCCGCCCAACATGTTC-3′ (the restriction enzyme sites are underlined), and cloned into the pET32a expression vector (Novagen). The construct was transformed into *E. coli* BL21 (DE3) cells for expression. M9 minimal medium containing $^{15}NH_4Cl$ (1 g L^{-1}) was used for ^{15}N-labeled protein expression. The fusion protein was expressed and purified initially using nickel-charged iminodiacetic acid chromatography. 3C protease (PreScission, Amersham Pharmacia Biotech) was used to remove the N-terminal fusion partner (thioredoxin-His_6-tag-S-tag), and the cleavage products were separated by reversed-phase HPLC. Unlabeled and ^{15}N-labeled N-BP-2 samples were prepared in this way. Protein samples were analyzed by polyacrylamide gel electrophoresis and quantified by reversed-phase HPLC. Electrospray mass spectroscopy was used to assess the isotope incorporation efficiency (>98%), and N-terminal sequencing confirmed that all preparations were of >95% purity. Full-length unlabeled IGFBP-2, IGF-I, and IGF-II for cross-linking analysis were purchased from Novozymes GroPep Ltd. (Adelaide, Australia). ^{125}I-labeled IGF-I and IGF-II were purchased from ProSearch, Australia. Low molecular weight heparin, with an average molecular mass of ∼3 kDa (∼12−15 monosaccharide units), was purchased from Sigma.

Affinity Cross-Linking. C-BP-2 (10 μg), N-BP-2 (0.5 μg), or IGFBP-2 (50 ng) was incubated with 5 ng of ^{125}I-IGF-I (200 000 cpm) ± excess unlabeled IGF-I at 4 °C for 16 h in 40 μL of PBS. Disuccinimidyl suberate was then added to the samples to a final concentration of 0.5 mM and incubated at 15 °C for 1 h. Cross-linking was terminated by the addition of Tris·HCl buffer (pH 7.5) to a concentration of 100 mM, followed by 5 min of incubation at 15 °C. The samples were then boiled for 5 min with electrophoresis loading buffer and separated on an SDS−15% polyacrylamide gel followed by autoradiography.

NMR Spectroscopy. NMR spectra were recorded on a Bruker Avance 500 spectrometer equipped with a cryoprobe. The spectra were referenced to an impurity peak at 0.15 ppm

in the ^{1}H dimension, which has been referenced previously against the internal standard dioxane (3.75 ppm) and does not vary with solution conditions over the pH and temperature ranges used in this study. The spectra were referenced indirectly using the experimentally determined frequency ratios for ^{15}N and ^{13}C (*36*). The spectra were processed using Topspin, version 1.3 (Bruker Biospin), and analyzed using XEASY, version 1.3 (*37*).

Unless otherwise stated, ^{15}N/^{13}C-labeled IGF-I titration experiments were performed in 95% H_2O/5% ^2H_2O containing 10 mM sodium acetate, 150 mM sodium chloride, and 0.02% (w/v) sodium azide, at pH 6.0 and 37 °C. The ^{1}H−^{15}N HSQC spectrum of a 0.05 mM ^{15}N/^{13}C-labeled IGF-I sample was recorded using a data matrix size of 2048 × 128 and with 256 scans per t_1 increment. The spectral widths were 12.0 ppm for ^{1}H and 35.0 ppm for ^{15}N; the carrier frequencies were 4.7 ppm for ^{1}H and 118 ppm for ^{15}N. Unlabeled C-BP-2 and N-BP-2 were then titrated into the ^{15}N/^{13}C-labeled IGF-I samples in separate experiments and ^{1}H−^{15}N HSQC spectra recorded at ^{15}N/^{13}C-IGF-I:C-BP-2 (or N-BP-2) ratios of 1:0.5, 1:1, and 1:1.5. Unlabeled C-BP-2 was then titrated into the ^{15}N/^{13}C-IGF-I + N-BP-2 (1:1.5) samples, and ^{1}H−^{15}N HSQC spectra were recorded at ^{15}N/^{13}C-IGF-I:N-BP-2:C-BP-2 ratios of 1:1.5:0.5, 1:1.5:1.0, and 1:1.5:1.5. ^{1}H−^{15}N HSQC spectra of IGF-I in the free form, binary complex (IGF-I:N-BP-2 = 1:1.5), and ternary complex (IGF-I:N-BP-2:C-BP-2 = 1:1.5:1.5) were also recorded at pH 4.0. ^{1}H−^{15}N HSQC spectra were recorded at ^{15}N/^{13}C-IGF-I:N-BP-2:C-BP-2 ratios of 1:1.5:0.5, 1:1.5:1.0, and 1:1.5:1.5. ^{1}H−^{15}N HSQC spectra of IGF-I in the ternary complex form were also recorded at pH 5.5, and at pH 6.0 and 5.5 in the presence of 2.0 mM low molecular weight heparin. Cross-peaks in the ^{1}H−^{15}N HSQC spectra of free IGF-I were assigned on the basis of 3D HNCA and CBCA(CO)NH spectra acquired on a 0.7 mM ^{15}N/^{13}C-IGF-I sample. Compared to those published previously (*38*, *39*), more complete assignments were obtained as a consequence of both improved sensitivity (use of a cryoprobe) and optimized solution conditions that minimized nonspecific aggregation (Kuang, et al., to be published). Assignments for IGF-I in the IGF-I·N-BP-2 binary complex and IGF-I·N-BP-2·C-BP-2 ternary complex were made using 3D HNCA and CBCA(CO)NH spectra acquired on these complexes with 0.2 mM ^{15}N/^{13}C-IGF-I.

^{1}H−^{15}N HSQC spectra of a 0.05 mM ^{15}N-labeled C-BP-2 sample were recorded as described above with 128 scans per t_1 increment. Unlabeled N-BP-2 was titrated into this sample, and the spectra were recorded at ^{15}N-C-BP-2:N-BP-2 ratios of 1:0.5 and 1:1. In the reverse experiment, ^{1}H−^{15}N HSQC spectra of ^{15}N-labeled N-BP-2 in the absence and presence of unlabeled C-BP-2 were recorded (further details are provided in the caption to Figure S3 in the Supporting Information).

RESULTS

IGF Interactions with C-BP-2 and N-BP-2. The interactions between IGF and individual domains of IGFBP-2 were assessed first using affinity cross-linking and then in detail by NMR spectroscopy. In the cross-linking experiments, ^{125}I-labeled IGF-I bound to C-BP-2, N-BP-2, and full-length IGFBP-2 (Figure 1). However, the IGF-I·C-BP-2 complex band was very weak compared to the IGF-I·IGFBP-2 or IGF-I·N-BP-2 band, even though the amount of C-BP-2 used in the interaction was approximately 20-fold more than that of N-BP-2 and 600-fold more than that of IGFBP-2 on a molar basis. Thus, on the basis of the band intensities and amounts of protein loaded, the IGF-I binding affinity of C-BP-2 was estimated to be >100-fold lower than that of N-BP-2 and >1000-fold lower than that of IGFBP-2. Similar results were obtained in ^{125}I-labeled IGF-II cross-linking experiments (Figure S1 in the Supporting Information).

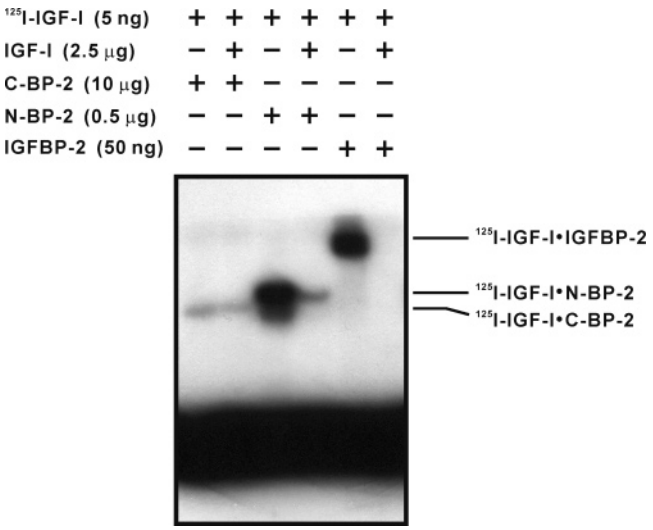

FIGURE 1: Binding of C-BP-2, N-BP-2, and IGFBP-2 to IGF-I was demonstrated by affinity cross-linking of these proteins to ^{125}I-labeled IGF-I. C-BP-2, N-BP-2, or IGFBP-2 was incubated with ^{125}I-IGF-I (200 000 cpm), with and without excess unlabeled IGF-I, at 4 °C overnight in 40 μL of PBS. Disuccinimidyl suberate was then used to cross-link the interacting proteins. The samples were separated on SDS−polyacrylamide gel, followed by autoradiography.

In NMR experiments, unlabeled C-BP-2 was titrated into ^{15}N/^{13}C-labeled IGF-I. The buffers contained 150 mM sodium chloride, and experiments were performed at 37 °C and pH 6.0. Previously, we have shown that IGFBP-2 binding to either IGF-I or IGF-II exhibited similar biosensor curves at pH 7.4, 6.4, and 5.4, but the dissociation from IGF was slightly faster at pH 4.4 and significantly faster at pH 3.4 (*38*). Therefore, our NMR study on IGF-I was conducted at pH 6, where IGFBP-2 binding was the same as at physiological pH, but self-association of IGF-I and amide exchange with solvent were less extensive, facilitating the recording of good-quality IGF-I spectra. ^{1}H−^{15}N HSQC spectra of ^{15}N/^{13}C-IGF-I in the free form and at IGF-I:C-BP-2 ratios of 1:1.5 at pH 6.0 are shown in Figure 2A. Titration of C-BP-2 caused gradual broadening and finally disappearance of specific IGF-I cross-peaks, indicating that the binding interaction was in the intermediate exchange regime on the NMR time scale (*40*). At an IGF-I:C-BP-2 ratio of 1:1.5, the ^{1}H−^{15}N cross-peaks of IGF-I residues Thr4, Gly7, Leu10, Phe16, Phe23, Phe25, Ile43, Asp45, and Phe49 had intensities <40% of those in free IGF-I, while those of Leu5, Cys6, Val11, Gly19, Tyr24, Val 44, Glu46, Cys47, Cys48, R50, Leu57, Tyr60, Cys61, and Ala62 were 40−60%. Cross-peaks of Asp12, Leu14, Leu15, Arg56, Leu64, Lys27, and Asp53 were significantly overlapped, and intensity changes could not be determined accurately. Those residues showing significant intensity changes are found on a continuous surface on one face of IGF-I, forming a

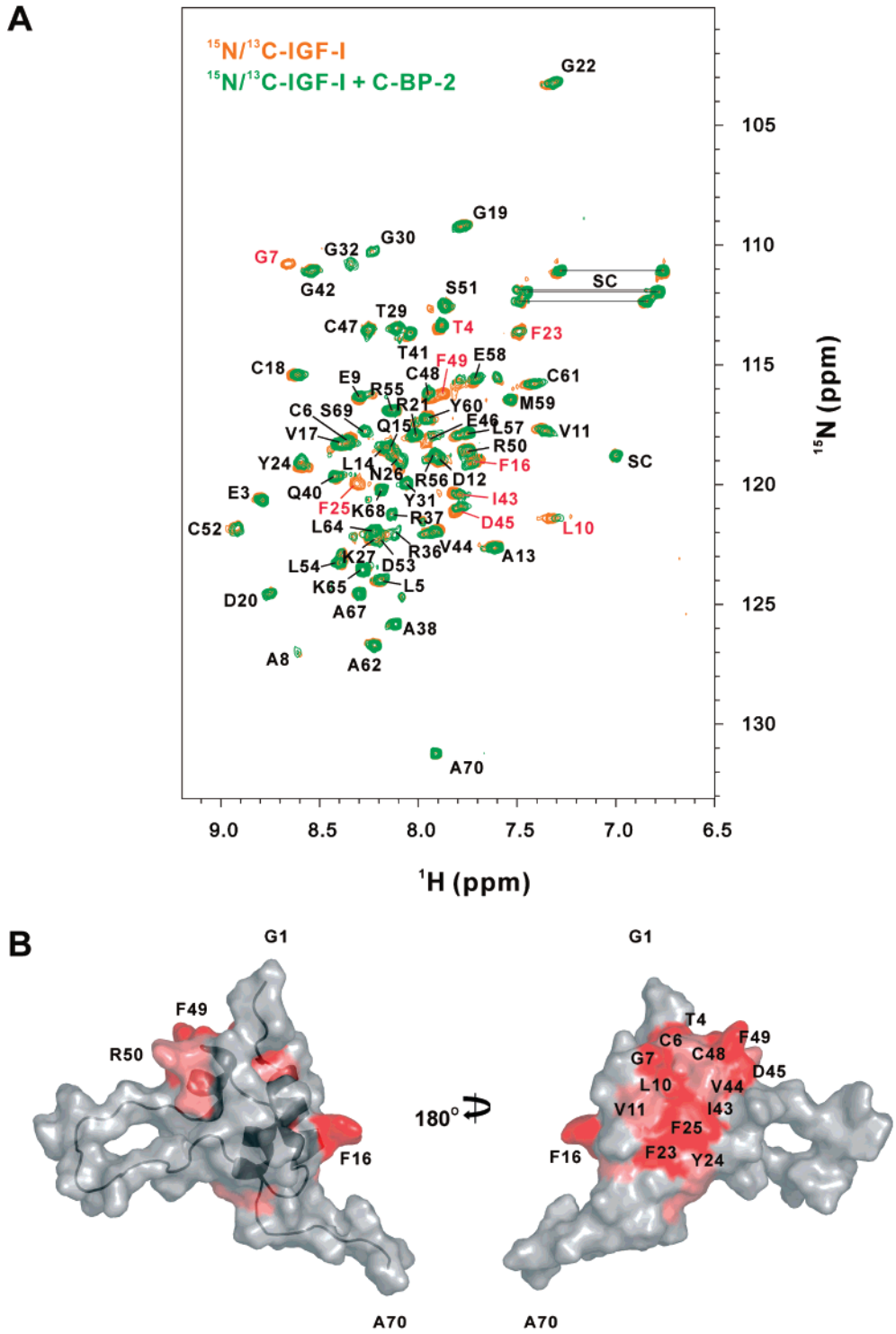

FIGURE 2: (A) Overlay of the ^{1}H−^{15}N HSQC spectra of 0.05 mM ^{15}N/^{13}C-labeled IGF-I in the absence (orange) and presence (green) of unlabeled C-BP-2 at IGF-I:C-BP-2 molar ratios of 1:1.5. The samples were in 95% H_2O/5% $^{2}H_2O$ containing 10 mM sodium acetate, 150 mM NaCl, and 0.02% (w/v) sodium azide at pH 6.0. The spectra were recorded at 500 MHz and 37 °C. Assignments of the free IGF-I cross-peaks are labeled, with those that retained <40% intensity in the presence of C-BP-2 being labeled in red. (B) Surface model of IGF-I (PDB 1PMX) (*62*) showing residues involved in C-BP-2 binding. Residues that retained <40% of the intensity of free IGF-I when bound to C-BP-2 in (A) are colored red, and those that retained >40% but <60% of the intensity of free IGF-I are in pink.

putativeC-BP-2 binding site (Figure 2B). The C-BP-2 binding site on IGF-I is consistent with the recent crystal structure of the IGF-I·N-BP-4·C-BP-4 ternary complex (*23*) and is equivalent to the C-BP-6 binding surface on IGF-II identified by NMR (*17*).

In contrast to the effects seen upon addition of C-BP-2, titrations of N-BP-2 at pH 6.0 caused a gradual disappearance of the "free" set of IGF-I cross-peaks and the simultaneous appearance of a "bound" set of cross-peaks (Figure 3A and Figure S2 in the Supporting Information). This indicated that the interaction between N-BP-2 and IGF-I was in the slow exchange regime on the NMR time scale (*40*) and thus was stronger than that between C-BP-2 and IGF-I, where intermediate exchange was observed.

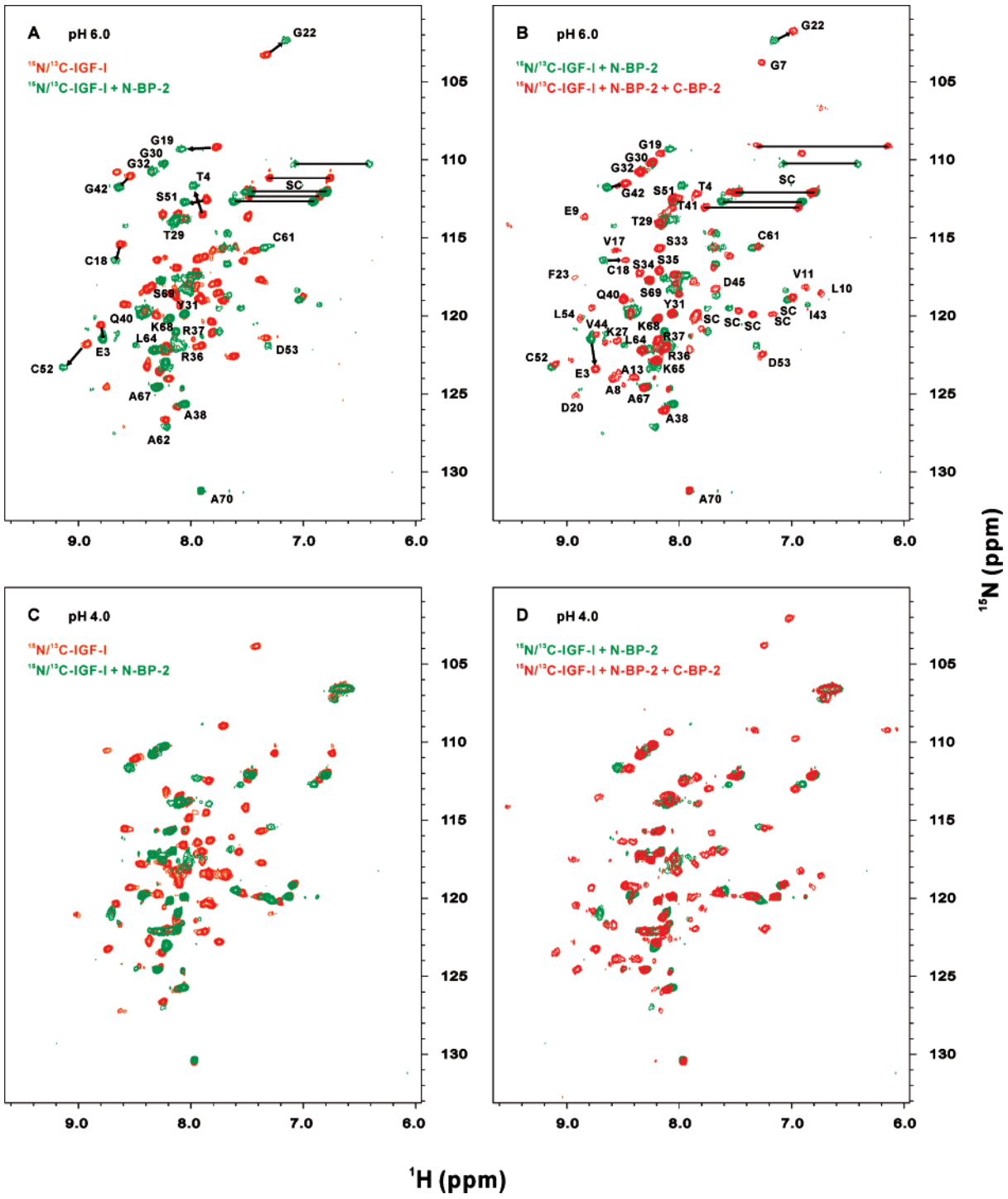

FIGURE 3: (A, C) Overlay of ^{1}H−^{15}N HSQC spectra of 0.05 mM ^{15}N/^{13}C-labeled IGF-I in the absence (orange) and presence (green) of unlabeled N-BP-2 at an IGF-I:N-BP-2 molar ratio of 1:1.5 at (A) pH 6.0 and (C) pH 4.0. (B, D) Overlay of ^{1}H−^{15}N HSQC spectra of 0.05 mM ^{15}N/^{13}C-labeled IGF-I in the presence of N-BP-2 alone (green) and of N-BP-2 plus C-BP-2 (red, at an IGF-I:N-BP-2:C-BP-2 molar ratio of 1:1.5:1.5) at (B) pH 6.0 and (D) pH 4.0. Assigned ^{1}H−^{15}N cross-peaks of IGF-I in complex with N-BP-2 (A) and with N-BP-2 plus C-BP-2 (B) are labeled. The samples were in 95% H_2O/5% $^{2}H_2O$ containing 10 mM sodium acetate, 150 mM NaCl, and 0.02% (w/v) sodium azide. The spectra were recorded at 500 MHz and 37 °C. Expanded views of selected regions of (A) and (B) are shown in Figure S2.

To compare the NMR results for IGF-I with the corresponding results for IGF-II obtained at pH 4.0 (Kuang et al., unpublished data), above which IGF-II gave very poor NMR spectra, ^{1}H−^{15}N HSQC spectra of IGF-I free and bound to N-BP-2 were also recorded at this pH (Figure 3C). While chemical shift changes of several IGF-I cross-peaks (e.g, Thr4 and Gly42) were seen at this pH, cross-peaks of many residues that shifted upon binding to N-BP-2 at pH 6.0 (Figure 3A) disappeared instead. This indicates that binding at pH 4.0 was weaker than at pH 6.0, shifting toward intermediate exchange for many resonances. This feature allowed us to observe the enhanced binding of N-BP-2 to IGF-I in the presence of C-BP-2, as described in the next section.

Interaction of the IGF·N-BP-2 Binary Complex with C-BP-2. When unlabeled C-BP-2 was titrated into the IGF-I·N-

BP-2 binary complex at pH 6.0, some IGF-I cross-peaks underwent further chemical shift changes in a slow exchange manner (Figure 3B and Figure S2 in the Supporting Information), indicating that binding of C-BP-2 to the IGF-I·N-BP-2 binary complex was significantly stronger than to IGF-I alone. $^{1}H-^{15}N$ HSQC spectra of $^{15}N/^{13}C$-labeled IGF-I in the ternary complex form were also recorded at pH 4.0 (Figure 3D); some cross-peaks that disappeared in the spectrum of the IGF-I·N-BP-2 binary complex at pH 4.0 due to intermediate exchange reappeared on a slow exchange basis, indicating stronger binding of N-BP-2 + C-BP-2 to IGF-I than that of N-BP-2 alone at pH 4.0. Thus, although at pH 6.0 the exchange frequency of IGF-I between the free and N-BP-2-bound forms could not be distinguished from that between the free form and the IGF-I·N-BP-2·C-BP-2 ternary complex form as both were in the slow exchange regime, they were distinguishable at pH 4.0 where C-BP-2 clearly stabilized the interaction between N-BP-2 and IGF-I. Therefore, the binding of N-BP-2 or C-BP-2 to IGF-I was enhanced in the presence of the other domain.

A comparison of the $^{1}H-^{15}N$ HSQC spectra of IGF-I in the IGF-I·N-BP-2 binary complex and the IGF-I·N-BP-2·C-BP-2 ternary complex with that of IGF-I in the IGF-I·IGFBP-2 complex (*38*) showed that IGF-I resonances in the IGF-I·N-BP-2·C-BP-2 ternary complex had chemical shifts very similar to those in the IGF-I·IGFBP-2 complex (Figure S3 in the Supporting Information). Therefore, N-BP-2 plus C-BP-2 fragments reconstituted the full binding site of IGFBP-2 for IGF-I, and IGF-I had essentially identical chemical environments in this ternary complex and the binary IGF·IGFBP-2 complex.

We also acquired 3D heteronuclear spectra using a more concentrated sample of $^{15}N/^{13}C$-IGF-I (0.2 mM) to assign the $^{1}H-^{15}N$ cross-peaks of IGF-I in the IGF-I·N-BP-2 binary and IGF-I·N-BP-2·C−BP-2 ternary complexes. We could assign 65% of the backbone amide $^{1}H-^{15}N$ cross-peaks of IGF-I in the IGF-I·N-BP-2·C-BP-2 ternary complex. However, cross-peak line widths of IGF-I in the higher concentration IGF-I·N-BP-2 binary complex were so broad that very poor signal-to-noise ratios were obtained in 3D spectra, and only a limited number of cross-peaks that shifted upon binding to N-BP-2 could be assigned. Nevertheless, some shifted peaks were close enough to their corresponding peaks in either free IGF-I or the IGF-I·N-BP-2·C-BP-2 ternary complex that they could be assigned as shown in Figure 3. The significantly sharper peak line widths of IGF-I in the higher concentration IGF-I·N-BP-2·C-BP-2 ternary complex sample compared to the IGF-I·N-BP-2 binary complex sample, even though the ternary complex has a higher molecular mass, further emphasized the stabilizing effect on the IGF-I conformation of having both domains present.

N-BP-2 Interaction with C-BP-2. Interactions between N-BP-2 and C-BP-2 in the absence of IGFs were investigated using both ^{15}N-labeled C-BP-2 and ^{15}N-labeled N-BP-2. Titration of unlabeled N-BP-2 into ^{15}N-labeled C-BP-2 caused significant broadening of many cross-peaks (Figure 4A). Some cross-peaks disappeared at a C-BP-2:N-BP-2 ratio of 1:0.5 (data not shown) and even more at a molar ratio of 1:1, although small chemical shift changes for some cross-peaks were also evident (Figure 4A). The most affected residues in C-BP-2 are located at the end of the helix (Arg206), loop I (Gly212, His216), the second β-sheet strand (Lys234, Lys237, Met238), and the second half of loop II (L240-Gly245) (Figure 4B). Addition of unlabeled C-BP-2 to ^{15}N-labeled N-BP-2 induced chemical shift changes and peak broadening of some cross-peaks (Figure S4 in the Supporting Information), further confirming the interaction between N-BP-2 and C-BP-2 even in the absence of IGFs.

Heparin Binding by the IGF-I·N-BP-2·C-BP-2 Ternary Complex. Addition of low molecular weight heparin to the $^{15}N/^{13}C$-IGF-I·N-BP-2·C-BP-2 ternary complex at pH 6.0 caused broadening and some chemical shift changes of IGF-I cross-peaks (Figure 5 and Figure S5 in the Supporting Information). When the pH was decreased to 5.5, peak broadening was more significant than at pH 6.0. Nevertheless, at pH 6.0 cross-peaks clearly had chemical shifts corresponding to IGF-I in the IGF-I·N-BP-2·C-BP-2 ternary complex, but not the IGF-I·N-BP-2 binary complex or the free form. Thus, these results suggested that the IGF-I·N-BP-2·C-BP-2 ternary complex can bind heparin, but that binding to heparin did not significantly dissociate the ternary complex. The chemical shift of Glu3 in IGF-I in the ternary complex was affected, more so at pH 5.5 than pH 6.0 (Figure 5), indicating that heparin bound to the pH-dependent C-BP-2 heparin binding site (*24*), which is predicted to be close to Glu3 of IGF-I in the ternary complex (Figure 4B,C). No change in Glu3 was observed when low molecular weight heparin was added to $^{15}N/^{13}C$-labeled IGF-I alone (Figure S6 in the Supporting Information). Heparin also affected the chemical shifts of Arg37 and Ala38 in the ternary complex (Figure 5), but addition of heparin to IGF-I alone also perturbed these chemical shifts (Figure S6). Thus, in addition to the heparin binding site on C-BP-2, low molecular weight heparin appeared to interact with the Arg36-Arg37-Ala38 region in the flexible C-domain of both the free and the ternary complex forms of IGF-I.

DISCUSSION

Cooperativity between N-BP-2 and C-BP-2 in IGF Binding. In this study, both affinity cross-linking and NMR results showed that the interaction between IGF and C-BP-2 is much weaker than that between IGF and IGFBP-2 or IGF and N-BP-2. The presence of N-BP-2 or C-BP-2 enhanced the affinity of the other domain for IGF-I, with the enhanced binding of C-BP-2 by N-BP-2 being more dramatic. These results help reconcile some of the discrepancies in the literature and address the question of why isolated C-domain fragments have low or even undetectable IGF binding ability, yet loss of the C-domain dramatically reduces IGF binding by IGFBPs. On the basis of these findings, studies of the IGF binding affinities of C-domains alone may not reflect their true IGF binding contribution in intact IGFBP molecules. It appears that the absence of the N-domain significantly reduces the IGF binding capacity of the C-domain. The results suggest that the IGF-I·C-BP-2 complex is either difficult to form or unstable. While IGF-I·N-BP binary complexes have been crystallized (*20*, *21*), no successful crystallization of an IGF·C-BP complex has been reported to date, although C-BP-4 has been crystallized with IGF-I and N-BP-4 in a ternary complex (*21*, *23*), which may reflect the differences observed here.

It is generally believed that covalently linking the N- and C-domain binding sites generates higher IGF binding affinity of IGFBPs than N-BP + C-BP, whereas limited proteolytic

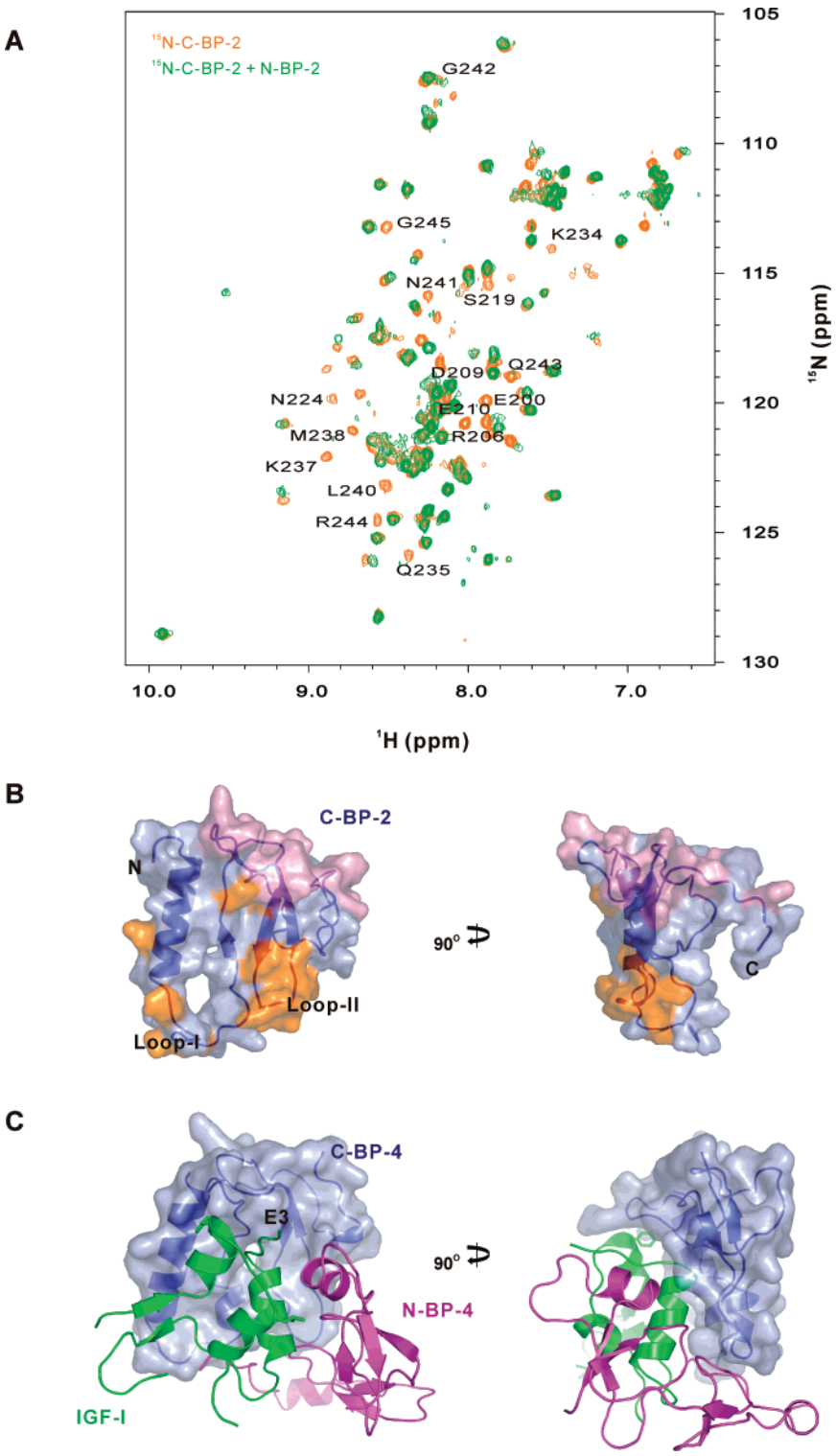

FIGURE 4: (A) Overlay of ^{1}H−^{15}N HSQC spectra of 0.05 mM ^{15}N-labeled C-BP-2 in the absence (orange) and presence (green) of unlabeled N-BP-2 at a C-BP-2:N-BP-2 molar ratio of 1:1. ^{1}H−^{15}N cross-peaks of C-BP-2 that disappeared upon binding to N-BP-2 are labeled. The samples were in 95% H_2O/5% $^{2}H_2O$ containing 10 mM sodium acetate, 150 mM NaCl, and 0.02% (w/v) sodium azide. The spectra were recorded at 500 MHz and 37 °C. (B) Surface model of C-BP-2 (PDB 2H7T) (*24*) showing residues whose ^{1}H−^{15}N cross-peaks disappeared upon N-BP-2 binding in orange. The heparin binding site on C-BP-2 identified by NMR (*24*) is colored light pink. (C) Crystal structure of the IGF-I•N-BP-4•C-BP-4 ternary complex (PDB 2DSR) (*23*). C-BP-4 is shown as a surface model and in an orientation equivalent to that of C-BP-2 in (B). N-BP-4 and IGF-I are shown as ribbon models. Residue Glu3 of IGF-I is indicated.

cleavages in the linker domain reduce binding affinity and release bound IGFs. However, previous investigations of cooperativity between the N- and C-domains of IGFBPs in IGF binding have been limited and controversial (*6*). No enhancement of IGF binding by co-incubation of the N- and C-domains of IGFBP-2 (*8*) or IGFBP-6 (*9*) was detected using surface plasmon resonance. In these assays one component of the complex was tethered to the biosensor surface, perhaps influencing the mechanism of complex formation. However, enhanced inhibition of IGF action by

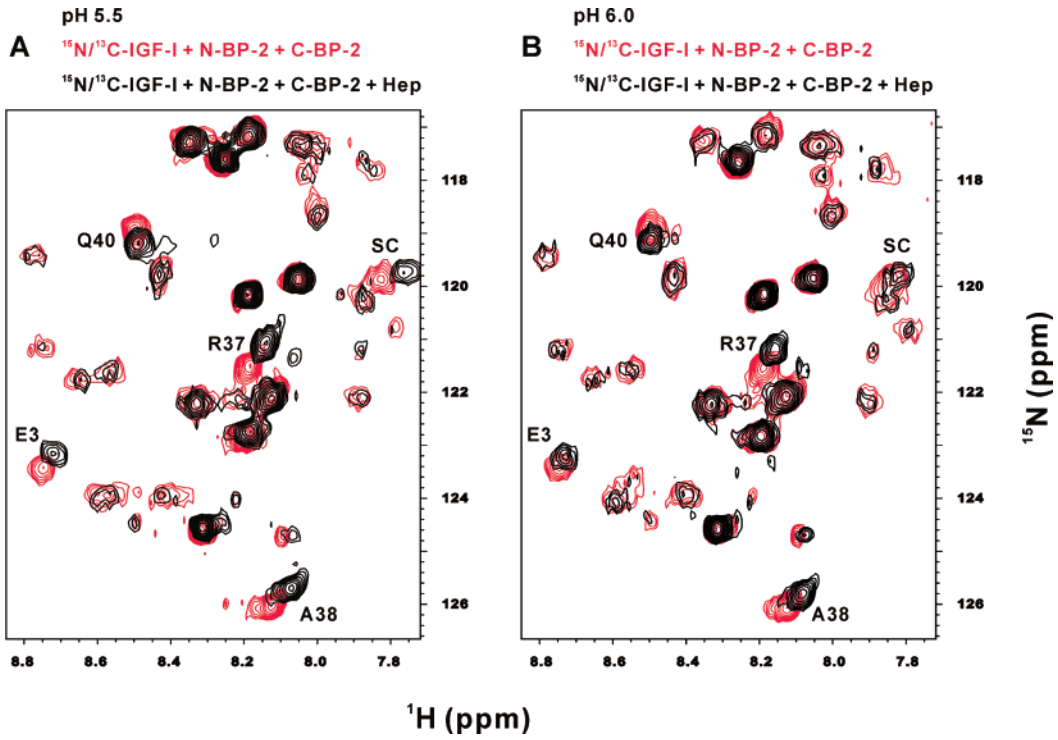

FIGURE 5: Overlay of ^{1}H−^{15}N HSQC spectra of 0.05 mM ^{15}N/^{13}C-labeled IGF-I in the IGF-I·N-BP-2·C-BP-2 ternary complex and in the absence (red) and presence (black) of 2.0 mM low molecular weight heparin at (A) pH 5.5 and (B) pH 6.0. The samples were in 95% H_2O/5% $^{2}H_2O$ containing 10 mM sodium acetate, 150 mM NaCl, and 0.02% (w/v) sodium azide. The spectra were recorded at 500 MHz and 37 °C. Full spectra are shown in Figure S4 in the Supporting Information. ^{1}H−^{15}N cross-peaks of IGF-I that shifted upon addition of low molecular weight heparin are labeled. Note that Gly1 and Pro2 do not have ^{1}H−^{15}N cross-peaks in the HSQC spectra.

the N- and C-domains of IGFBP-6 was also not seen (*9*). In contrast, Payet and co-workers demonstrated a strong cooperative effect of the IGFBP-3 N- and C-domain fragments in IGF binding using solution binding assays with affinity-tagged domains (*28*). Even a 25-fold excess of either N-BP-3 or C-BP-3 alone had minimal inhibition of IGF-stimulated DNA synthesis, but N-BP-3 + C-BP-3 had only a 5-fold lower inhibitory effect than intact IGFBP-3 (*28*). A synergistic effect was also reported in a study of N- and C-domain fragments of IGFBP-4 using isothermal titration calorimetry (*21*); C-BP-4 bound to the IGF-I·N-BP-4 binary complex but not to IGF-I alone, and the presence of C-BP-4 also increased the affinity of N-BP-4 for IGF-I (*21*). No underlying mechanisms were described in those studies, and wild-type binding affinities were not achieved by combining individual domains.

In our study, the cooperativity between N-BP-2 and C-BP-2 was clearly evident when the NMR resonance perturbation patterns in different interactions were compared. Our data also suggest possible reasons for this cooperativity (see below). On the basis of the corresponding IGF-I spectra, IGF-I residues had essentially identical chemical environments in the IGF-I·N-BP-2·C-BP-2 ternary and IGF-I·IGFBP-2 binary complexes (Figure S3 in the Supporting Information). The NMR data suggested that both IGFBP-2 and N-BP-2 + C-BP-2 bound IGF-I with high affinities and were in the slow exchange regime on the NMR time scale. However, the binding constants for these strong interactions (K_d < μM) could not be quantified by NMR; while quantitative measures can be obtained if the K_d is within an order of magnitude of the concentration of the studied species, the protein concentrations required for the experiments exceed this range (*40*).

Conformational Changes of IGF-I. One possible mechanism for the cooperativity is that the IGF molecules and/or the N- and C-domains undergo conformational changes upon binding to one partner that generate a higher affinity conformation for the other partner. Crystal structures of the free and N-BP-bound IGF-I (*20*, *21*, *23*, *41*, *42*), in conjunction with the NMR data presented here, provide insight into possible conformational changes in the ligand.

In chemical shift perturbation mapping, both a direct contact with the binding partner and a conformational change induced by binding can perturb resonances (*40*). When unlabeled N-BP-2 was titrated into ^{15}N-labeled IGF-I at pH 6.0, it caused chemical shift changes of a large number of IGF-I cross-peaks (Figure 3A). Cross-peaks from Gly30−Arg36 and Lys65−Ala70, which are located in the flexible C- or D-domain, respectively, did not change, but cross-peaks of some residues in the A1 helix (Ile43−Phe49) were perturbed significantly. However, in the reported IGF-I·N-BP structures (*20*, *21*, *23*) IGF-I residues Ile43−Phe49 were not close to the IGF-I·N-BP binding interfaces (Figure 6A). In Figure 6B,C, crystal structures of free IGF-I (bound to detergent molecules) (*41*, *42*), the IGF-I·mini-N-BP-5 binary complex (*20*), and the IGF-I·N−BP-4·C−BP-4 ternary complex (*23*) are superimposed over backbone heavy atoms of the three helices. It can be seen that the spatial organization of the helices and the structure of residues Ile43−Glu46 did not change significantly upon binding to mini-N-BP-5 or N-BP-4 + C-BP-4. However, IGF-I residues Phe49−Leu54, as well as the Phe49 aromatic ring, adopted a conformation in the IGF-I·mini-N-BP-5 and IGF-I·N-BP-4·C-BP-4 complexes significantly different from that in free IGF-I.

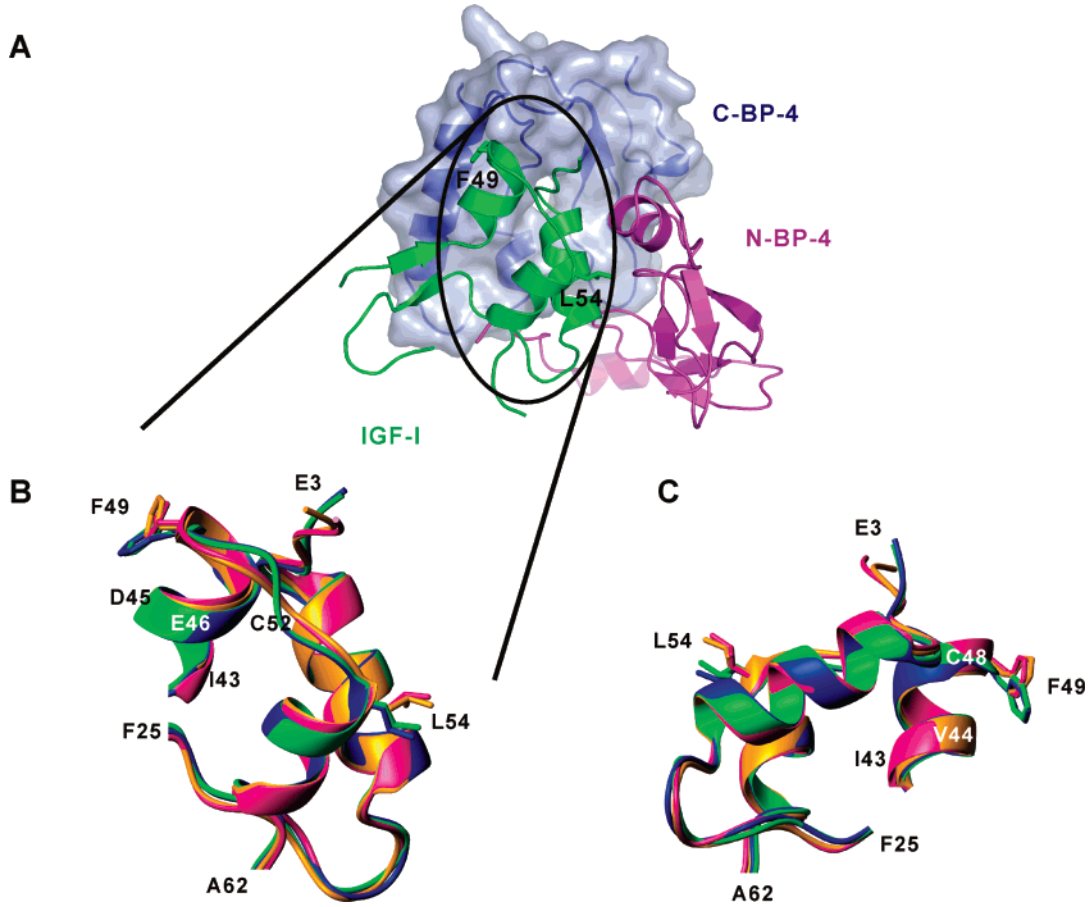

FIGURE 6: (A) Crystal structure of the IGF-I·N-BP-4·C-BP-4 ternary complex (PDB 2DSR) (*23*). Residues Phe49 and Leu54 of IGF-I are labeled. (B, C) Superposition of IGF-I crystal structures showing conformational changes upon binding to N-domains. Ribbon views of IGF-I in the free form (bound to detergent molecules), PDB 1GZR (blue) (*42*) and PDB 1IMX (green) (*41*), the IGF-I·mini-N-BP-5 binary complex (PDB 1H59, orange) (*20*), and the IGF-I·N-BP-4·C−BP-4 ternary complex (PDB 2DSR, deep pink) (*23*) are superimposed over backbone heavy atoms of the three helices (Ala8−Cys18, Gly42−Cys48, Leu54−Cys61). The side chains of Phe49 and Leu54 are shown. The structures are shown in two different orientations (B, C). The structures in (B) are in an orientation equivalent to that of the IGF-I structure in (A). Parts of the flexible regions that do not contact either the N-domain or C-domain (residues 1−2, 26−42, and 63−70) are excluded for clarity. The four crystal structures (*20*, *23*, *41*, *42*) used in the comparison were of high resolution, and the regions of Phe49−Leu54 and the Phe49 ring were well defined (Supporting Information Table S1).

It is possible that the significant chemical shift perturbations of IGF-I residues Ile43−Glu46 upon binding to N-BP-2 were caused by a conformational change of the Phe49 aromatic ring through "ring current" effects (*43*). Previous NMR studies have shown significant internal flexibility of IGF-I (*44*−*46*) and IGF-II (*47*, *48*) molecules. The conformations of Phe49−Leu54 and the Phe49 side chain in IGF-I, as well as the equivalent residues in IGF-II, in these NMR structures were not well defined, probably resulting from flexibility in this region together with low NMR spectral quality due to aggregation. In NMR binding experiments, the free and bound sets of cross-peaks represent the average conformations of these two states in solution. Thus, the NMR data suggest that the conformational differences around Phe49−Leu54 between free and N-BP-bound IGF-I seen in the crystal structures may exist in solution.

It appears that the interaction between the IGFBP N-domain and IGF-I is strong and is sufficient to either induce a conformational change in IGF-I or selectively stabilize the IGF-I in the bound conformation. On the other hand, the interaction between the IGFBP C-domain and free IGF-I is weak, possibly due to low complementarity between the free form of the Phe49 side chain and the IGF binding site on the C-domain. IGF-I residue Phe49 and the IGF-II equivalent Phe48 are very important for IGFBP binding (*49*−*52*). IGF·C-BP interactions may be too weak to either induce the conformational change or stabilize IGF in the bound conformation. However, when IGF-I is bound to the N-domain, its C-domain binding site, and especially the Phe49 side chain, could be stabilized in a conformation that binds the C-domain with high affinity. In return, binding of the C-domain to this site may further stabilize the bound conformation of IGF-I and thus reciprocally enhance the interaction between IGF-I and the N-domain. Thus, the Phe49−Leu54 region of IGF-I may mediate the cooperativity between the N- and C-domains, with the N-domain interacting at the Leu54 end while the C-domain interacts at the Phe49 end.

Interdomain Interaction between IGFBP-2 N- and C-Domains. Interaction between C-BP-2 and N-BP-2 could also contribute to the observed stronger binding of C-BP-2 to the IGF-I·N-BP-2 complex than that to IGF-I alone. While N-BP-2 and C-BP-2 may undergo local conformational changes upon binding to IGF that enhance their binding to one another, our NMR results using both ^{15}N-labeled C-BP-2 and ^{15}N-labeled N-BP-2 show that N-BP-2 and C-BP-2 also interact with each other in the absence of IGFs. The interdomain interaction between IGFBP N- and C-domains

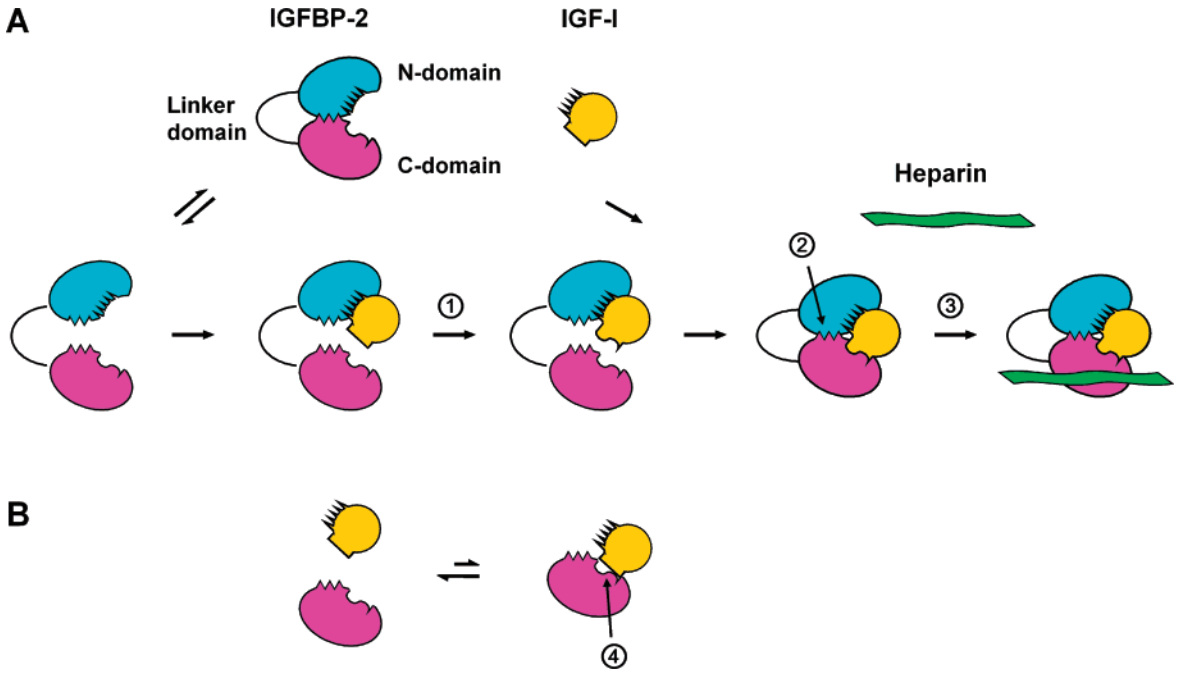

FIGURE 7: Schematic representation of (A) formation of the IGF-I·IGFBP-2 complex and heparin binding to the complex and (B) interaction between IGF-I and the proteolytic IGFBP-2 C-domain fragments (1). Conformational change of the IGFBP-2 C-domain binding site on IGF-I upon its binding to the N-domain (2). Interdomain interaction between N- and C-domains of IGFBP-2 (3). Heparin binding to the IGF-I·IGFBP-2 complex. In addition to its binding site on C-BP-2, heparin also appears to interact with the Arg36-Arg37-Ala38 region of IGF-I (not shown in this diagram) (4). There is less structural complementarity in the binding interface between the C-domain and IGF-I in the absence of the N-domain.

in the absence of IGF has not been detected previously (*21*, *28*). The N-BP-2 binding site on C-BP-2 identified by NMR largely correlated with the C-BP-4 surface contacting N-BP-4 in the IGF-I·N-BP-4·C-BP-4 ternary complex structure reported recently (*23*). In both cases the interaction is mainly mediated by the loop II and loop I regions (Figure 4). Therefore, the direct interaction between N-BP-2 and C-BP-2 revealed by NMR appears to be biologically relevant.

While previous studies suggested that the N- and C-domains were close to each other or even in contact in the IGF·IGFBP complex (*8*, *17*, *21*, *23*), little was known regarding the spatial organization of the N- and C-domains in the free form of IGFBPs. Since we have detected interdomain interactions in the absence of IGFs, the N- and C-domains may be contacting each other in ligand-free IGFBP-2. However, this interaction does not seem to be strong or stable, as it was not detected in other assays (*28*) and would be unlikely to hinder IGF access to the N- and C-domain binding sites. The significant flexibility in the interdomain binding sites, i.e., the loop II and loop I regions of the C-domains (*18*, *24*), would enable large conformational changes and domain movements upon IGF binding. The linker domain is also believed to be flexible, thus allowing interdomain movement upon ligand binding (*3*, *6*).

Effect of Heparin Binding on the Ternary Complex. We recently described a pH-dependent heparin binding site on C-BP-2 (*24*). This binding occurs at slightly acidic pH (6.0) and is more significant at pH 5.5, but is largely suppressed at pH 7.4 (*24*). Having established that N-BP-2 + C-BP-2 mimicked IGFBP-2 in IGF binding, it was of interest to study the effect of heparin binding on the IGF·IGFBP interaction using these domain fragments. We found that the IGF-I·N-BP-2·C-BP-2 ternary complex bound to low molecular weight heparin and that the interaction resulted in the formation of larger complexes rather than dissociation of the IGF-I·N-BP-2·C-BP-2 complex, as IGF-I $^{1}H-^{15}N$ cross-peaks were broadened but still represented the ternary complex form and not the N-BP-2-bound binary complex form. On the basis of the locations of the IGF and N-BP-2 binding sites and the IGF-I·N-BP-4·C-BP-C structure (*23*), the C-BP-2 heparin binding site (*24*) is expected to be accessible in the IGF-I·N-BP-2·C-BP-2 ternary complex (Figure 4), and heparin binding to this site may not significantly interfere with IGF binding. Indeed, addition of low molecular weight heparin to the ternary complex affected the $^{1}H-^{15}N$ cross-peak of Glu3 in IGF-I, which is predicted to be close to the C-BP-2 heparin binding site; the perturbation was larger at pH 5.5 than pH 6.0 (Figure 5).

Previous data regarding glycosaminoglycan binding by IGFBP-2 and its effect on IGF binding have been controversial. Arai and co-workers reported that heparin did not inhibit IGF·IGFBP-2 binding (*53*), and heparin only bound IGFBP-2 when it was complexed to IGF (*32*). Russo and co-workers reported that binding of IGFBP-2 to chondroitin 6-sulfate decreased the binding affinity of IGFBP-2 for IGF-I approximately 3-fold (*33*). It is worth noting that small to moderate changes in binding constants may not be detected in the current NMR experiments if the binding interaction remained in the same chemical exchange regime. Further investigations are warranted to establish whether IGF binding and heparin binding by IGFBP-2 enhance or (slightly) compete with each other. IGFBP-2 is markedly overexpressed in many malignancies (*54*, *55*), but there is only limited evidence so far that demonstrates its role in promoting cancer growth (*54*, *56*). Previously, we suggested that IGFBP-2 or IGF·IGFBP-2 complexes might preferentially bind to glycosaminoglycans in acidic tumor ECM, but not in neutral, normal tissue ECM (*24*). Current results suggest

that binding of IGF•IGFBP-2 complexes to glycosaminoglycans per se may not result in IGF release. Nevertheless, many tumors overexpress IGFBP-cleaving proteases (*57*), so unbound IGFs and RGD-containing IGFBP-2 C-domain fragments may accumulate in tumor ECM due to enhanced glycosaminoglycan binding and limited proteolysis. In contrast, heparin binding by IGFBP-5 reduced its IGF-I binding by 17-fold (*53*), and strong competition between IGF and heparin binding by IGFBP-3 and -5 was demonstrated by both BIAcore and solution binding assays (*58*). These significant differences highlight the specific IGF-dependent and IGF-independent actions of different IGFBPs.

Concluding Remarks. We have employed different isotopic labeling schemes to study the molecular interactions among three partners, the N- and C-domains of IGFBP-2 and IGF-I. We have detected cooperativity between the N- and C-domains in IGF-I binding and described two possible mechanisms that might contribute to this phenomenon. These findings are summarized schematically in Figure 7. Many protein−protein interactions are mediated by two or more domains in one protein. For example, insulin and IGF receptors have multiple ligand binding sites on different domains that cooperate to achieve high-affinity ligand binding (*4*). While it is a common approach to subdivide large proteins into individual domains and study interactions between domains in binary complexes (especially for NMR studies, where size restrictions may obtain), our results emphasize the importance of analyzing the relationships among two or more binding sites in an integrated manner. Similar mechanisms may also contribute to other molecular interactions; for example, conformational changes of insulin upon binding to its receptor have been reported (*59*−*61*). Future structural and biophysical studies on how IGFs bind to IGFBP N- and C-domains, which are smaller and easier to study compared with domains of insulin/IGF receptors, may serve as a model in understanding other multidomain molecular interactions.

ACKNOWLEDGMENT

We thank Dr. Chris Bagley and Mr. Chris Cursaro, Adelaide Proteomics Facility, for mass spectrometry and N-terminal sequencing.

SUPPORTING INFORMATION AVAILABLE

NMR and other data referred to in the text. This material is available free of charge via the Internet at http://pubs.acs.org.

REFERENCES

1. Pollak, M. N., Schernhammer, E. S., and Hankinson, S. E. (2004) Insulin-like growth factors and neoplasia, *Nat. Rev. Cancer 4*, 505−518.
2. Ranke, M. B. (2005) Insulin-like growth factor-I treatment of growth disorders, diabetes mellitus and insulin resistance, *Trends Endocrinol. Metab. 16*, 190−197.
3. Firth, S. M., and Baxter, R. C. (2002) Cellular actions of the insulin-like growth factor binding proteins, *Endocr. Rev. 23*, 824−854.
4. Denley, A., Cosgrove, L. J., Booker, G. W., Wallace, J. C., and Forbes, B. E. (2005) Molecular interactions of the IGF system, *Cytokine Growth Factor Rev. 16*, 421−439.
5. Hwa, V., Oh, Y., and Rosenfeld, R. G. (1999) The insulin-like growth factor-binding protein (IGFBP) superfamily, *Endocr. Rev. 20*, 761−787.
6. Bach, L. A., Headey, S. J., and Norton, R. S. (2005) IGF-binding proteins−the pieces are falling into place, *Trends Endocrinol. Metab. 16*, 228−234.
7. Carrick, F. E., Wallace, J. C., and Forbes, B. E. (2002) The interaction of insulin-like growth factor (IGFs) with insulin-like growth factor binding proteins (IGFBPs): a review, *Lett. Pept. Sci. 8*, 147−153.
8. Carrick, F. E., Forbes, B. E., and Wallace, J. C. (2001) BIAcore analysis of bovine insulin-like growth factor (IGF)-binding protein-2 identifies major IGF binding site determinants in both the amino- and carboxyl-terminal domains, *J. Biol. Chem. 276*, 27120−27128.
9. Headey, S. J., Leeding, K. S., Norton, R. S., and Bach, L. A. (2004) Contributions of the N- and C-terminal domains of insulin-like growth factor (IGF) binding protein-6 to IGF binding, *J. Mol. Endocrinol. 33*, 377−386.
10. Forbes, B. E., Turner, D., Hodge, S. J., McNeil, K. A., Forsberg, G., and Wallace, J. C. (1998) Localization of an insulin-like growth factor (IGF) binding site of bovine IGF binding protein-2 using disulfide mapping and deletion mutation analysis of the C-terminal domain, *J. Biol. Chem. 273*, 4647−4652.
11. Clemmons, D. R. (2001) Use of mutagenesis to probe IGF-binding protein structure/function relationships, *Endocr. Rev. 22*, 800−817.
12. Shand, J. H., Beattie, J., Song, H., Phillips, K., Kelly, S. M., Flint, D. J., and Allan, G. J. (2003) Specific amino acid substitutions determine the differential contribution of the N- and C-terminal domains of insulin-like growth factor (IGF)-binding protein-5 in binding IGF-I, *J. Biol. Chem. 278*, 17859−17866.
13. Yan, X., Forbes, B. E., McNeil, K. A., Baxter, R. C., and Firth, S. M. (2004) Role of N- and C-terminal residues of insulin-like growth factor (IGF)-binding protein-3 in regulating IGF complex formation and receptor activation, *J. Biol. Chem. 279*, 53232−53240.
14. Horney, M. J., Evangelista, C. A., and Rosenzweig, S. A. (2001) Synthesis and characterization of insulin-like growth factor (IGF)-1 photoprobes selective for the IGF-binding proteins (IGFBPS). photoaffinity labeling of the IGF-binding domain on IGFBP-2, *J. Biol. Chem. 276*, 2880−2889.
15. Kibbey, M. M., Jameson, M. J., Eaton, E. M., and Rosenzweig, S. A. (2006) Insulin-like growth factor binding protein-2: contributions of the C-terminal domain to IGF-1 binding, *Mol. Pharmacol. 69*, 833−845.
16. Headey, S. J., Keizer, D. W., Yao, S., Brasier, G., Kantharidis, P., Bach, L. A., and Norton, R. S. (2004) C-terminal domain of insulin-like growth factor (IGF) binding protein-6: structure and interaction with IGF-II, *Mol. Endocrinol. 18*, 2740−2750.
17. Headey, S. J., Keizer, D. W., Yao, S., Wallace, J. C., Bach, L. A., and Norton, R. S. (2004) Binding site for the C-domain of insulin-like growth factor (IGF) binding protein-6 on IGF-II; implications for inhibition of IGF actions, *FEBS Lett. 568*, 19−22.
18. Yao, S., Headey, S. J., Keizer, D. W., Bach, L. A., and Norton, R. S. (2004) C-terminal domain of insulin-like growth factor (IGF) binding protein 6: conformational exchange and its correlation with IGF-II binding, *Biochemistry 43*, 11187−11195.
19. Kalus, W., Zweckstetter, M., Renner, C., Sanchez, Y., Georgescu, J., Grol, M., Demuth, D., Schumacher, R., Dony, C., Lang, K., and Holak, T. A. (1998) Structure of the IGF-binding domain of the insulin-like growth factor-binding protein-5 (IGFBP-5): implications for IGF and IGF-I receptor interactions, *EMBO J. 17*, 6558−6572.
20. Zesławski, W., Beisel, H. G., Kamionka, M., Kalus, W., Engh, R. A., Huber, R., Lang, K., and Holak, T. A. (2001) The interaction of insulin-like growth factor-I with the N-terminal domain of IGFBP-5, *EMBO J. 20*, 3638−3644.
21. Siwanowicz, I., Popowicz, G. M., Wisniewska, M., Huber, R., Kuenkele, K. P., Lang, K., Engh, R. A., and Holak, T. A. (2005) Structural basis for the regulation of insulin-like growth factors by IGF binding proteins, *Structure (London) 13*, 155−167.
22. Sala, A., Capaldi, S., Campagnoli, M., Faggion, B., Labo, S., Perduca, M., Romano, A., Carrizo, M. E., Valli, M., Visai, L., Minchiotti, L., Galliano, M., and Monaco, H. L. (2005) Structure and properties of the C-terminal domain of insulin-like growth factor-binding protein-1 isolated from human amniotic fluid, *J. Biol. Chem. 280*, 29812−29819.
23. Sitar, T., Popowicz, G. M., Siwanowicz, I., Huber, R., and Holak, T. A. (2006) Structural basis for the inhibition of insulin-like

growth factors by insulin-like growth factor-binding proteins, *Proc. Natl. Acad. Sci. U.S.A. 103*, 13028−13033.
24. Kuang, Z., Yao, S., Keizer, D. W., Wang, C. C., Bach, L. A., Forbes, B. E., Wallace, J. C., and Norton, R. S. (2006) Structure, dynamics and heparin binding of the C-terminal domain of insulin-like growth factor-binding protein-2 (IGFBP-2), *J. Mol. Biol. 364*, 690−704.
25. Chandrashekaran, I. R., Yao, S., Wang, C. C., Bansal, P. S., Alewood, P. F., Forbes, B. E., Wallace, J. C., Bach, L. A., and Norton, R. S. (2007) The N-terminal subdomain of insulin-like growth factor (IGF) binding protein 6. Structure and interaction with IGFs, *Biochemistry 46*, 3065−3074.
26. Ho, P. J., and Baxter, R. C. (1997) Characterization of truncated insulin-like growth factor-binding protein-2 in human milk, *Endocrinology 138*, 3811−3818.
27. Vorwerk, P., Hohmann, B., Oh, Y., Rosenfeld, R. G., and Shymko, R. M. (2002) Binding properties of insulin-like growth factor binding protein-3 (IGFBP-3), IGFBP-3 N- and C-terminal fragments, and structurally related proteins mac25 and connective tissue growth factor measured using a biosensor, *Endocrinology 143*, 1677−1685.
28. Payet, L. D., Wang, X. H., Baxter, R. C., and Firth, S. M. (2003) Amino- and carboxyl-terminal fragments of insulin-like growth factor (IGF) binding protein-3 cooperate to bind IGFs with high affinity and inhibit IGF receptor interactions, *Endocrinology 144*, 2797−2806.
29. Mark, S., Kubler, B., Honing, S., Oesterreicher, S., John, H., Braulke, T., Forssmann, W. G., and Standker, L. (2005) Diversity of human insulin-like growth factor (IGF) binding protein-2 fragments in plasma: primary structure, IGF-binding properties, and disulfide bonding pattern, *Biochemistry 44*, 3644−3652.
30. Qin, X., Strong, D. D., Baylink, D. J., and Mohan, S. (1998) Structure-function analysis of the human insulin-like growth factor binding protein-4, *J. Biol. Chem. 273*, 23509−23516.
31. Fernandez-Tornero, C., Lozano, R. M., Rivas, G., Jimenez, M. A., Standker, L., Diaz-Gonzalez, D., Forssmann, W. G., Cuevas, P., Romero, A., and Gimenez-Gallego, G. (2005) Synthesis of the blood circulating C-terminal fragment of insulin-like growth factor (IGF)-binding protein-4 in its native conformation. Crystallization, heparin and IGF binding, and osteogenic activity, *J. Biol. Chem. 280*, 18899−18907.
32. Arai, T., Busby, W., Jr., and Clemmons, D. R. (1996) Binding of insulin-like growth factor (IGF) I or II to IGF-binding protein-2 enables it to bind to heparin and extracellular matrix, *Endocrinology 137*, 4571−4575.
33. Russo, V. C., Bach, L. A., Fosang, A. J., Baker, N. L., and Werther, G. A. (1997) Insulin-like growth factor binding protein-2 binds to cell surface proteoglycans in the rat brain olfactory bulb, *Endocrinology 138*, 4858−4867.
34. Song, H., Shand, J. H., Beattie, J., Flint, D. J., and Allan, G. J. (2001) The carboxy-terminal domain of IGF-binding protein-5 inhibits heparin binding to a site in the central domain, *J. Mol. Endocrinol. 26*, 229−239.
35. King, R., Wells, J. R., Krieg, P., Snoswell, M., Brazier, J., Bagley, C. J., Wallace, J. C., Ballard, F. J., Ross, M., and Francis, G. L. (1992) Production and characterization of recombinant insulin-like growth factor-I (IGF-I) and potent analogues of IGF-I, with Gly or Arg substituted for Glu3, following their expression in Escherichia coli as fusion proteins, *J. Mol. Endocrinol. 8*, 29−41.
36. Wishart, D. S., Bigam, C. G., Yao, J., Abildgaard, F., Dyson, H. J., Oldfield, E., Markley, J. L., and Sykes, B. D. (1995) ^{1}H, ^{13}C and ^{15}N chemical shift referencing in biomolecular NMR, *J. Biomol. NMR 6*, 135−140.
37. Bartels, C., Xia, T. H., Billeter, M., Güntert, P., and Wüthrich, K. (1995) The program XEASY for computer-supported NMR spectral-analysis of biological macromolecules, *J. Biomol. NMR 6*, 1−10.
38. Carrick, F. E., Hinds, M. G., McNeil, K. A., Wallace, J. C., Forbes, B. E., and Norton, R. S. (2005) Interaction of insulin-like growth factor (IGF)-I and -II with IGF binding protein-2: mapping the binding surfaces by nuclear magnetic resonance, *J. Mol. Endocrinol. 34*, 685−698.
39. Denley, A., Wang, C. C., McNeil, K. A., Walenkamp, M. J., van Duyvenvoorde, H., Wit, J. M., Wallace, J. C., Norton, R. S., Karperien, M., and Forbes, B. E. (2005) Structural and functional characteristics of the Val44Met insulin-like growth factor I missense mutation: correlation with effects on growth and development, *Mol. Endocrinol. 19*, 711−721.
40. Zuiderweg, E. R. (2002) Mapping protein-protein interactions in solution by NMR spectroscopy, *Biochemistry 41*, 1−7.
41. Vajdos, F. F., Ultsch, M., Schaffer, M. L., Deshayes, K. D., Liu, J., Skelton, N. J., and de Vos, A. M. (2001) Crystal structure of human insulin-like growth factor-1: detergent binding inhibits binding protein interactions, *Biochemistry 40*, 11022−11029.
42. Brzozowski, A. M., Dodson, E. J., Dodson, G. G., Murshudov, G. N., Verma, C., Turkenburg, J. P., de Bree, F. M., and Dauter, Z. (2002) Structural origins of the functional divergence of human insulin-like growth factor-I and insulin, *Biochemistry 41*, 9389−9397.
43. Haigh, C. W., and Mallion, R. B. (1979) Ring current theories in nuclear magnetic resonance, *Prog. NMR Spectrosc. 13*, 303−344.
44. Cooke, R. M., Harvey, T. S., and Campbell, I. D. (1991) Solution structure of human insulin-like growth factor-I: a nuclear magnetic resonance and restrained molecular dynamics study, *Biochemistry 30*, 5484−5491.
45. Laajoki, L. G., Francis, G. L., Wallace, J. C., Carver, J. A., and Keniry, M. A. (2000) Solution structure and backbone dynamics of long-[Arg(3)]insulin-like growth factor-I, *J. Biol. Chem. 275*, 10009−10015.
46. Sato, A., Nishimura, S., Ohkubo, T., Kyogoku, Y., Koyama, S., Kobayashi, M., Yasuda, T., and Kobayashi, Y. (1993) Three-dimensional structure of human insulin-like growth factor-I (IGF-I) determined by ^{1}H-NMR and distance geometry, *Int. J. Pept. Protein Res. 41*, 433−440.
47. Terasawa, H., Kohda, D., Hatanaka, H., Nagata, K., Higashihashi, N., Fujiwara, H., Sakano, K., and Inagaki, F. (1994) Solution structure of human insulin-like growth factor II; recognition sites for receptors and binding proteins, *EMBO J. 13*, 5590−5597.
48. Torres, A. M., Forbes, B. E., Aplin, S. E., Wallace, J. C., Francis, G. L., and Norton, R. S. (1995) Solution structure of human insulin-like growth factor II. Relationship to receptor and binding protein interactions, *J. Mol. Biol. 248*, 385−401.
49. Clemmons, D. R., Dehoff, M. L., Busby, W. H., Bayne, M. L., and Cascieri, M. A. (1992) Competition for binding to insulin-like growth factor (IGF) binding protein-2, 3, 4, and 5 by the IGFs and IGF analogs, *Endocrinology 131*, 890−895.
50. Oh, Y., Mueller, H. L., Lee, D. Y., Fielder, P. J., and Rosenfeld, R. G. (1993) Characterization of the affinities of insulin-like growth factor (IGF)-binding protein -1 to -4 for IGF-I, IGF-II, IGF-I/insulin hybrid, and IGF-I analogs, *Endocrinology 132*, 1337−1344.
51. Dubaquie, Y., and Lowman, H. B. (1999) Total alanine-scanning mutagenesis of insulin-like growth factor I (IGF-I) identifies differential binding epitopes for IGFBP-1 and IGFBP-3, *Biochemistry 38*, 6386−6396.
52. Bach, L. A., Hsieh, S., Sakano, K., Fujiwara, H., Perdue, J. F., and Rechler, M. M. (1993) Binding of mutants of human insulin-like growth factor II to insulin-like growth factor binding proteins 1−6, *J. Biol. Chem. 268*, 9246−9254.
53. Arai, T., Parker, A., Busby, W., Jr., and Clemmons, D. R. (1994) Heparin, heparan sulfate, and dermatan sulfate regulate formation of the insulin-like growth factor-I and insulin-like growth factor-binding protein complexes, *J. Biol. Chem. 269*, 20388−20393.
54. Hoeflich, A., Reisinger, R., Lahm, H., Kiess, W., Blum, W. F., Kolb, H. J., Weber, M. M., and Wolf, E. (2001) Insulin-like growth factor-binding protein 2 in tumorigenesis: protector or promoter?, *Cancer Res. 61*, 8601−8610.
55. Zhang, W., Wang, H., Song, S. W., and Fuller, G. N. (2002) Insulin-like growth factor binding protein 2: gene expression microarrays and the hypothesis-generation paradigm, *Brain Pathol. 12*, 87−94.
56. Fukushima, T., Tezuka, T., Shimomura, T., Nakano, S., and Kataoka, H. (2007) Silencing of insulin-like growth factor binding protein-2 (IGFBP-2) in human glioblastoma cells reduces both invasiveness and expression of progression-associated gene CD24, *J. Biol. Chem. 282*, 18634−18644.
57. Bunn, R. C., and Fowlkes, J. L. (2003) Insulin-like growth factor binding protein proteolysis, *Trends Endocrinol. Metab. 14*, 176−181.
58. Beattie, J., Phillips, K., Shand, J. H., Szymanowska, M., Flint, D. J., and Allan, G. J. (2005) Molecular recognition characteristics

in the insulin-like growth factor (IGF)-insulin-like growth factor binding protein -3/5 (IGFBP-3/5) heparin axis, *J. Mol. Endocrinol. 34*, 163−175.

59. Hua, Q. X., Shoelson, S. E., Kochoyan, M., and Weiss, M. A. (1991) Receptor binding redefined by a structural switch in a mutant human insulin, *Nature 354*, 238−241.
60. Dong, J., Wan, Z., Popov, M., Carey, P. R., and Weiss, M. A. (2003) Insulin assembly damps conformational fluctuations: Raman analysis of amide I linewidths in native states and fibrils, *J. Mol. Biol. 330*, 431−442.
61. Hua, Q. X., Nakagawa, S., Hu, S. Q., Jia, W., Wang, S., and Weiss, M. A. (2006) Toward the active conformation of insulin: stereospecific modulation of a structural switch in the B chain, *J. Biol. Chem. 281*, 24900−24909.
62. Schaffer, M. L., Deshayes, K., Nakamura, G., Sidhu, S., and Skelton, N. J. (2003) Complex with a phage display-derived peptide provides insight into the function of insulin-like growth factor I, *Biochemistry 42*, 9324−9334.

BI701251D